Research on beamformation of low frequency radio telescope array for pulsar observation

Yukai Zhou
Supervisor: Youling Yue, Weiwei Zhu, Renxin Xu
Collaborator: Mengyao Xue, Chunfeng Zhang, Chao Wang, Cijie Zhang, Qiuyang Fu, Jiayi Liang, et al.

2024.7.14

0. 21CMA

Figure 1. Photograph of the east–west baseline of the 21CMA, in which the building to the left is the control center. (**武向平** 2019; C. Zheng, Wu, and Johnston-Hollitt 2015; Q. Zheng et al. 2016)

0. 21CMA

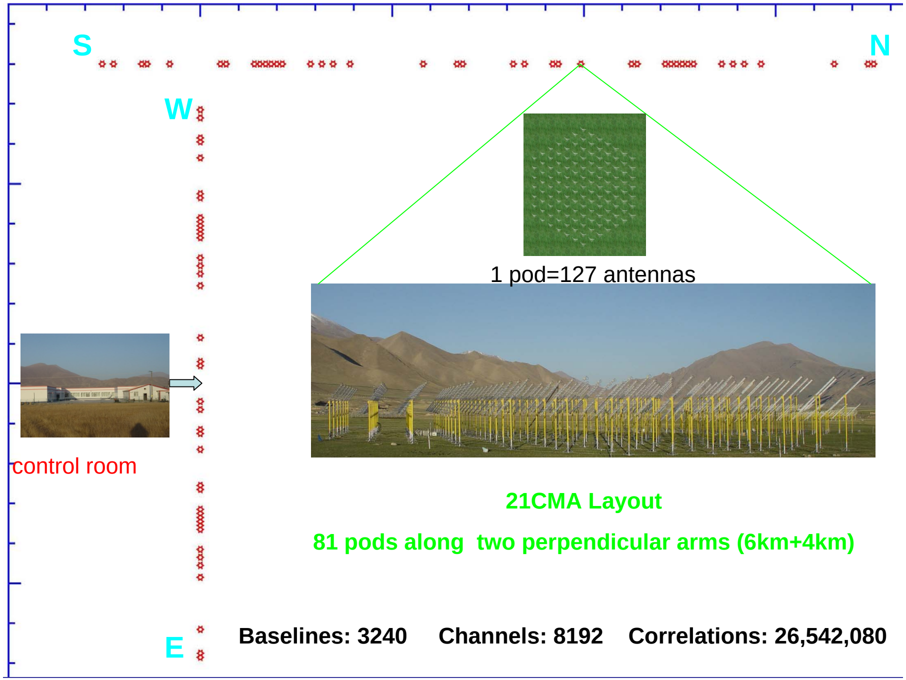

Figure 2. Locations of stations of 21CMA (武向平 2019; C. Zheng, Wu, and Johnston-Hollitt 2015)

0. 21CMA

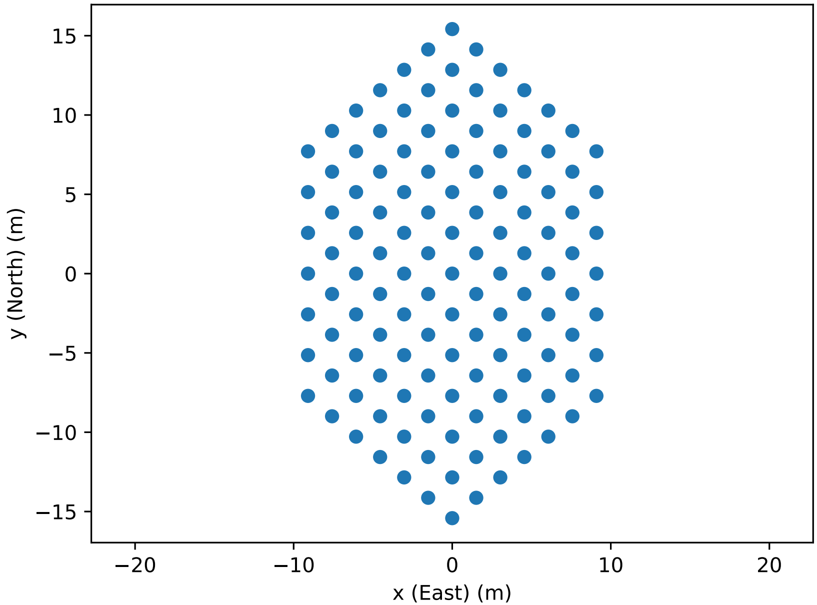

Figure 3. Layout of a single station, each point represents a log-periodic antenna

1. Pulsar Backend

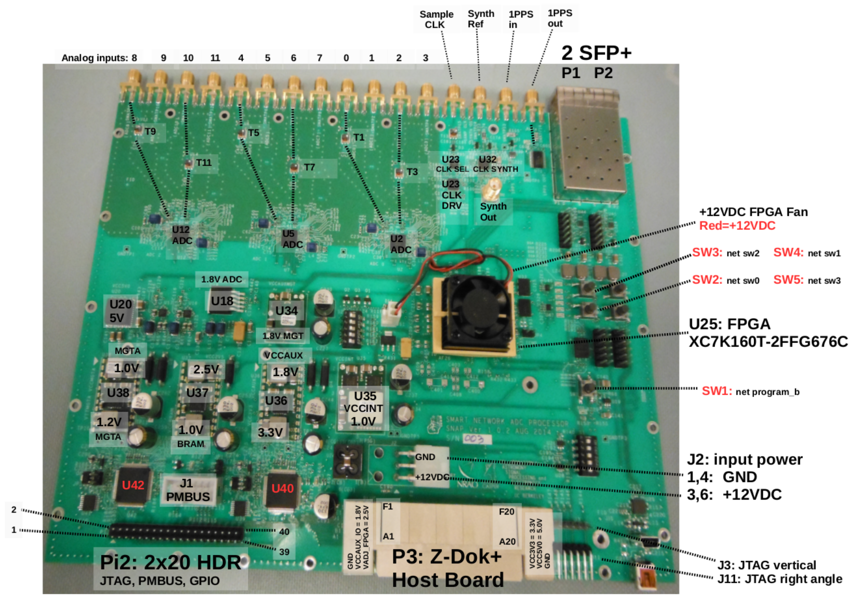

Figure 4. Overview of SNAP (DeBoer et al. 2020)

- 4 × 8 bit 409.6 Msps, 50 – 200 MHz effective
- direct sampling & baseband output

1. Pulsar Backend

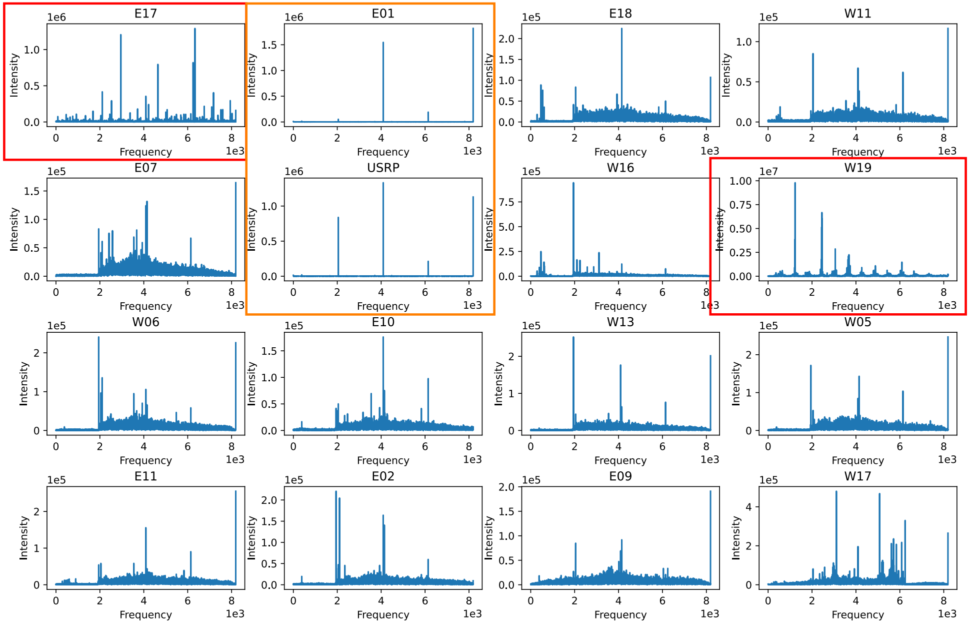

Figure 5. Spectrum of related arrays at UTC 2024-02-26 10:00:00, x-axis: frequency channel, 8192 channels of 0 - 204.8 MHz, y-axis: intensity (not calibrated), stations labeled red: broken on this time point, stations labeled orange: no signal

1. Pulsar Backend

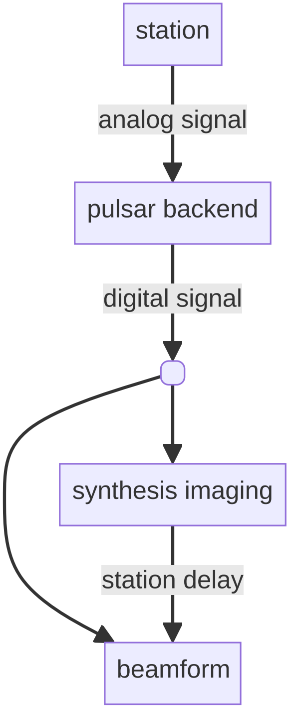

Figure 6. Schematic of data flow

2. Synthesis Imaging: to get delay of stations

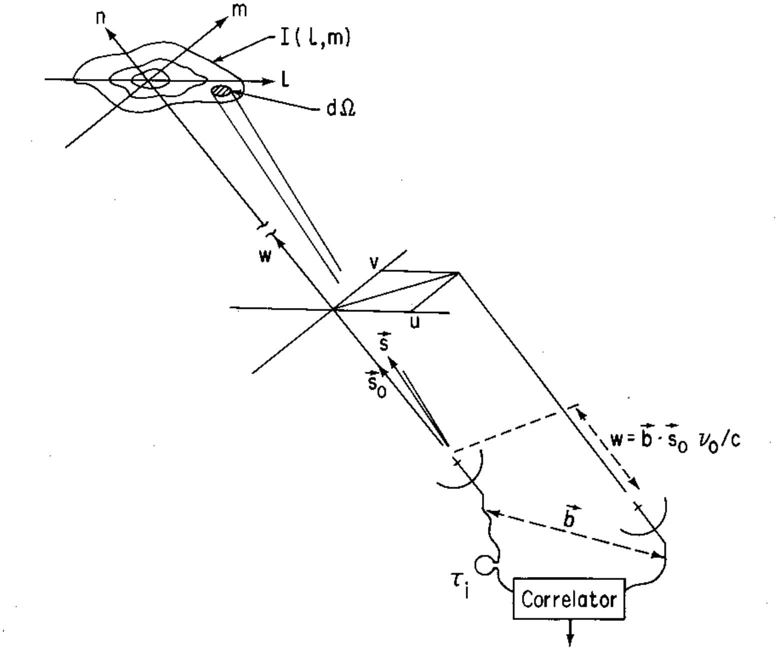

Figure 7. Schematic of synthesis imaging (Thompson 1999)

2. Synthesis Imaging: to get delay of stations

Signal correlation

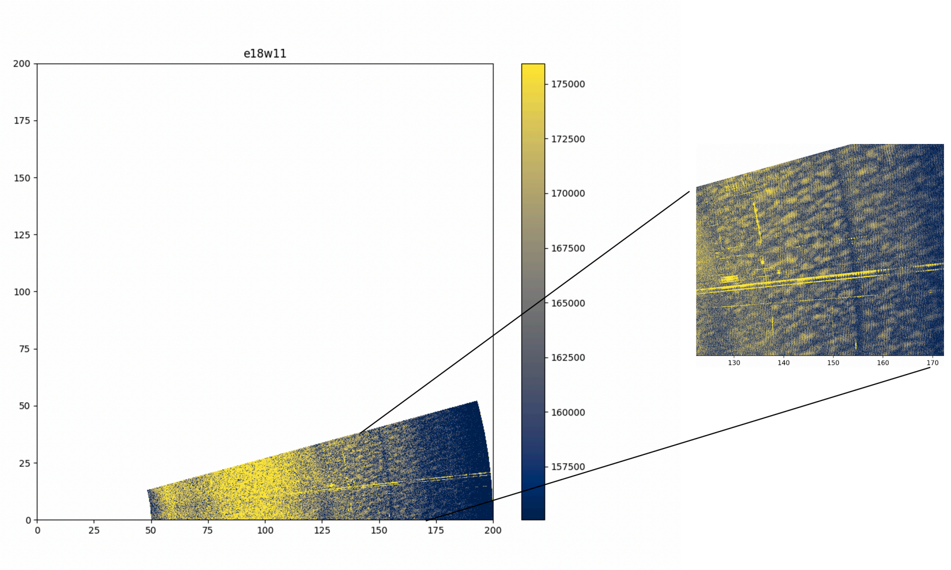

Figure 8. Testing E18 – W11 signal correlation (梁嘉一 2024)

2. Synthesis Imaging: to get delay of stations

Manual Optimizing Delay

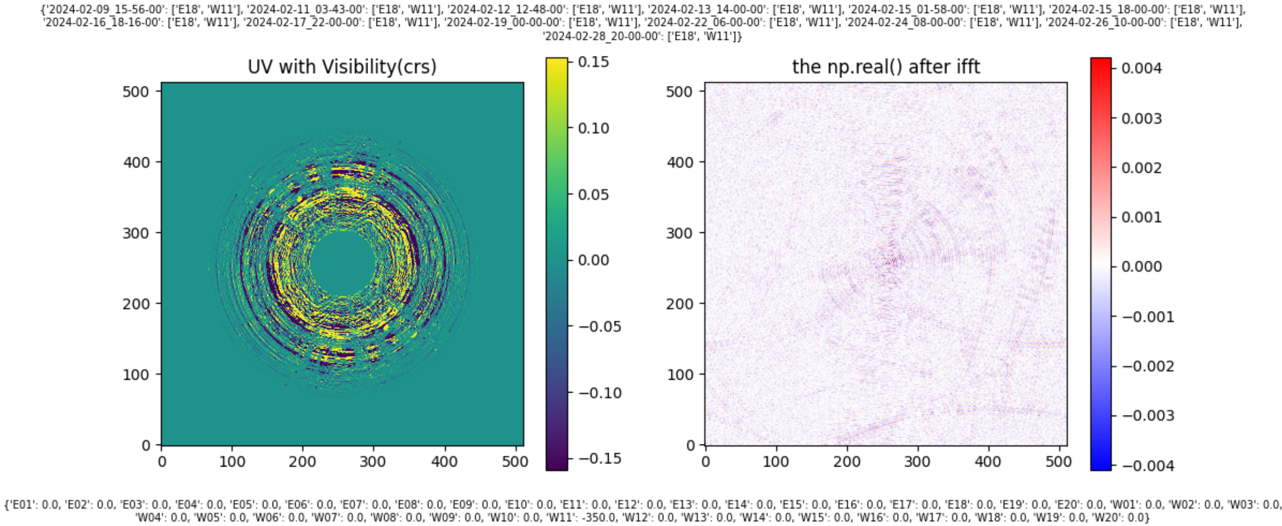

Figure 9. Synthesis imaging using E18 – W11 baseline, with relative delay -350 m.

2. Synthesis Imaging: to get delay of stations

Manual Optimizing Delay

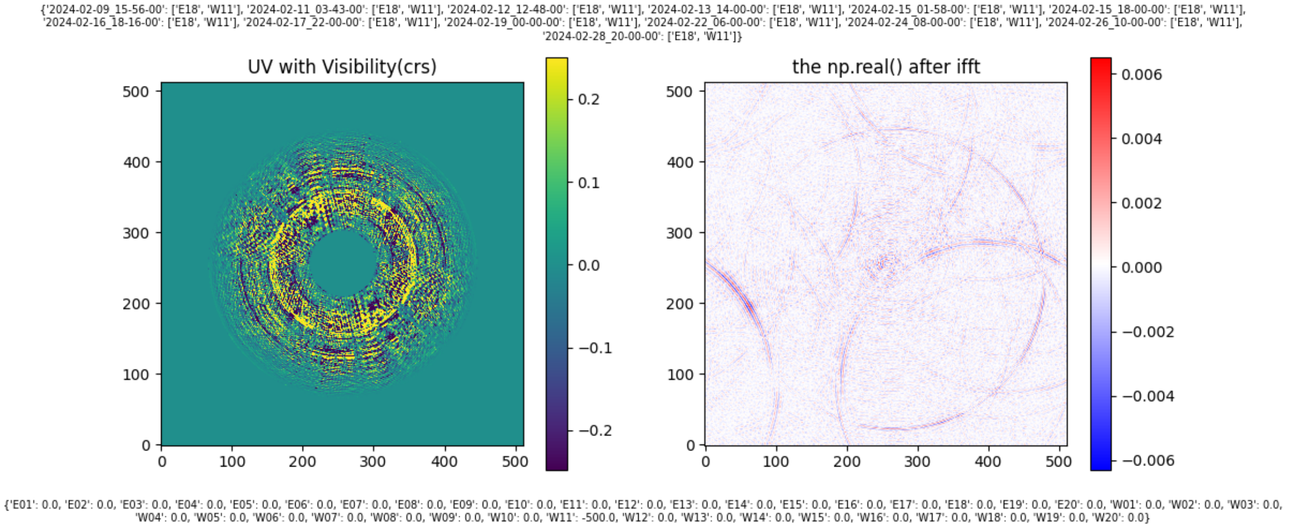

Figure 10. Synthesis imaging using E18 – W11 baseline, with relative delay -500 m.

2. Synthesis Imaging: to get delay of stations

Manual Optimizing Delay

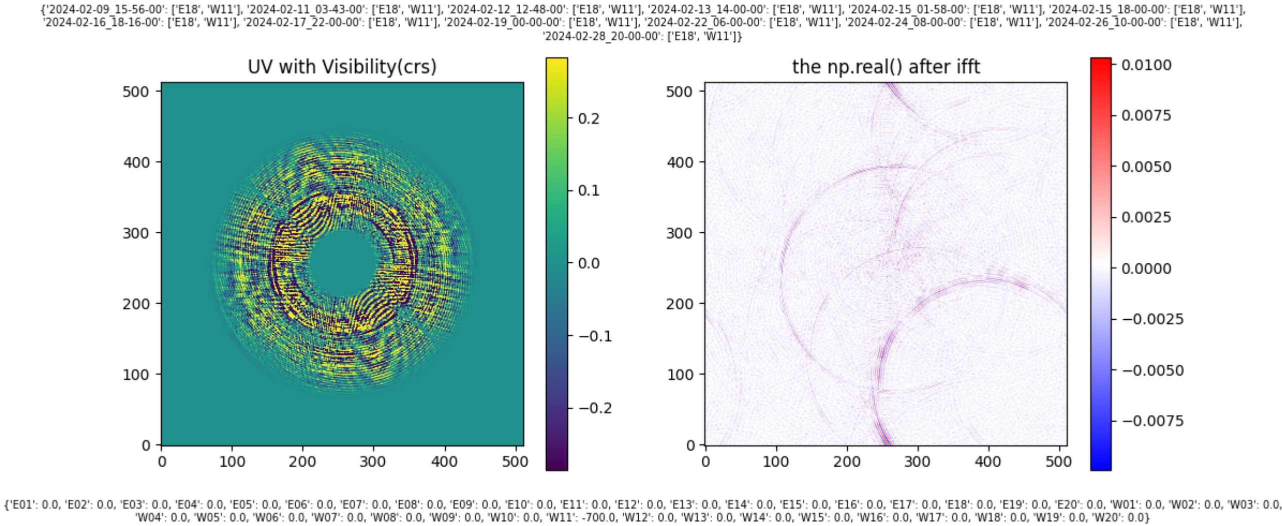

Figure 11. Synthesis imaging using E18 – W11 baseline, with relative delay -700 m.

2. Synthesis Imaging: to get delay of stations

Manual Optimizing Delay

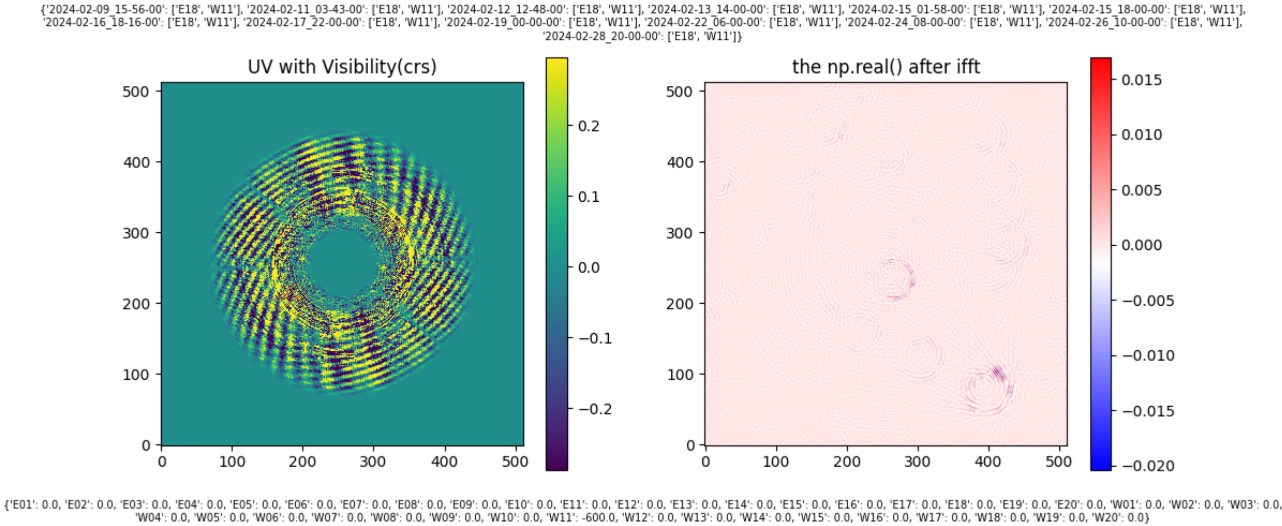

Figure 12. Synthesis imaging using E18 – W11 baseline, with relative delay -600 m.

2. Synthesis Imaging: to get delay of stations

Manual Optimizing Delay

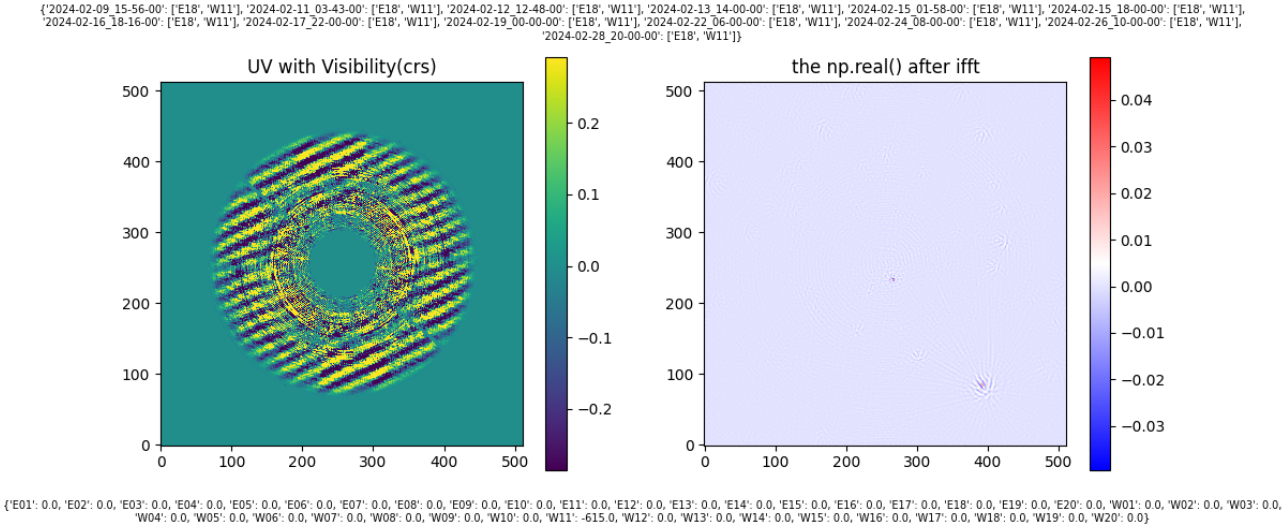

Figure 13. Synthesis imaging using E18 – W11 baseline, with relative delay -615 m.

2. Synthesis Imaging: to get delay of stations

Imaging of north celestial pole

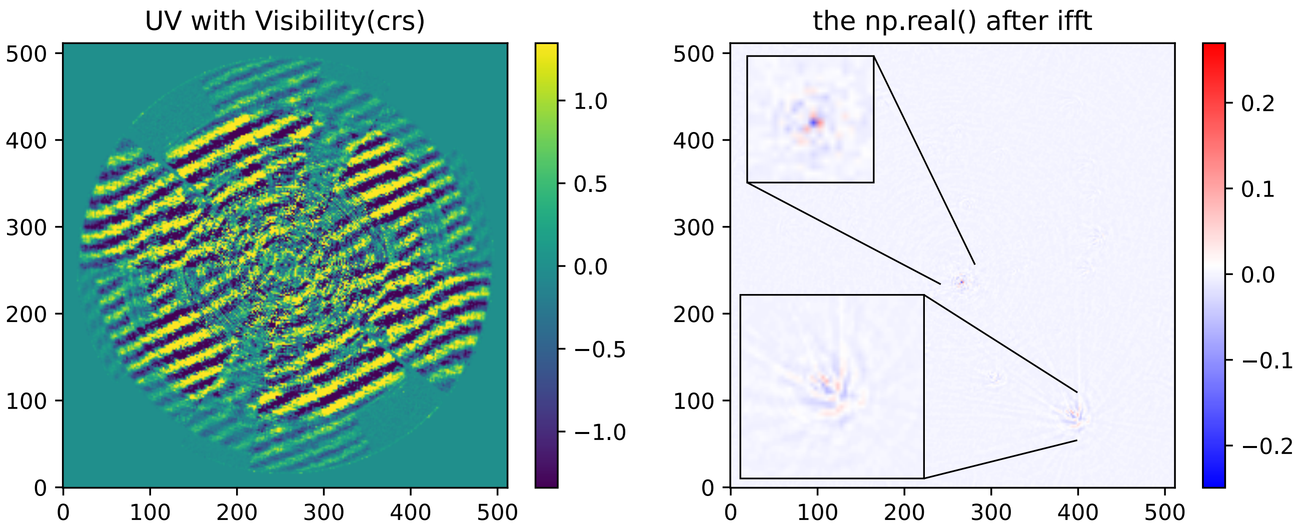

Figure 14. Synthesis imaging of north celestial pole after manual and auto optimization of delays between all available stations, $14 \times 13/2 = 91$ baselines in total. Left: UV coverage and visibility; Right: image of north celestial pole;

2. Synthesis Imaging: to get delay of stations

Imaging of north celestial pole

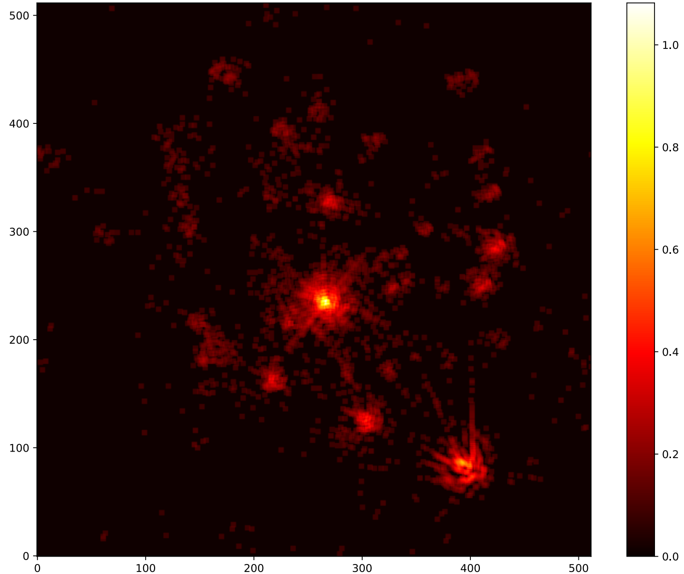

Figure 15. 50 – 200 MHz CLEAN-ed image of north celestial pole, using original simple CLEAN code on fig. 14, data from 14 stations

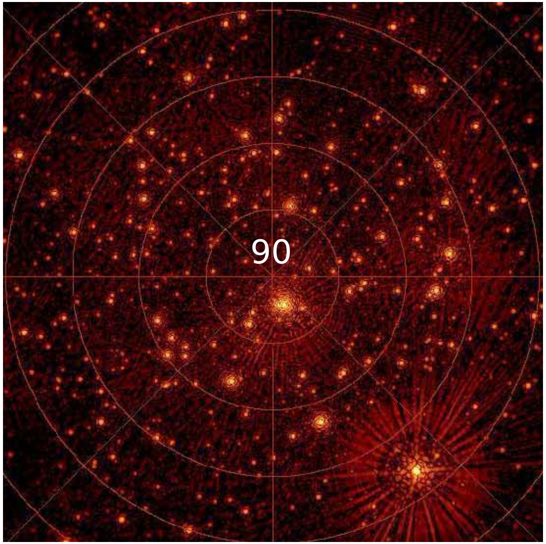

Figure 16. Reference 75 – 175 MHz dirty image of north celestial pole (Q. Zheng et al. 2016), cut to focus on center region, data from 40 stations

2. Synthesis Imaging: to get delay of stations

Imaging of north celestial pole

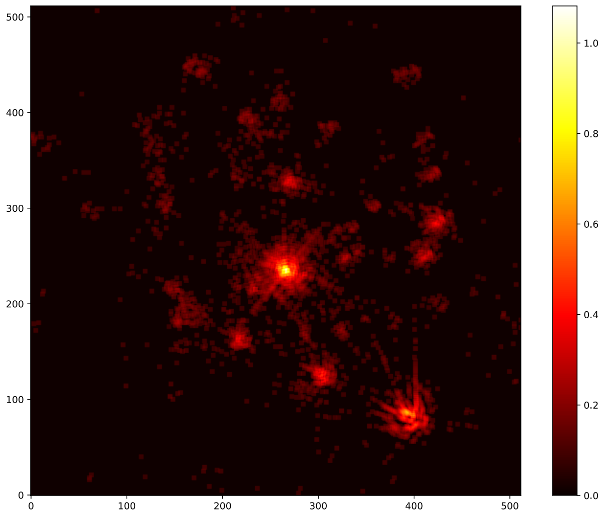

Figure 17. 50 – 200 MHz CLEAN-ed image of north celestial pole, using original simple CLEAN code on fig. 14, data from 14 stations

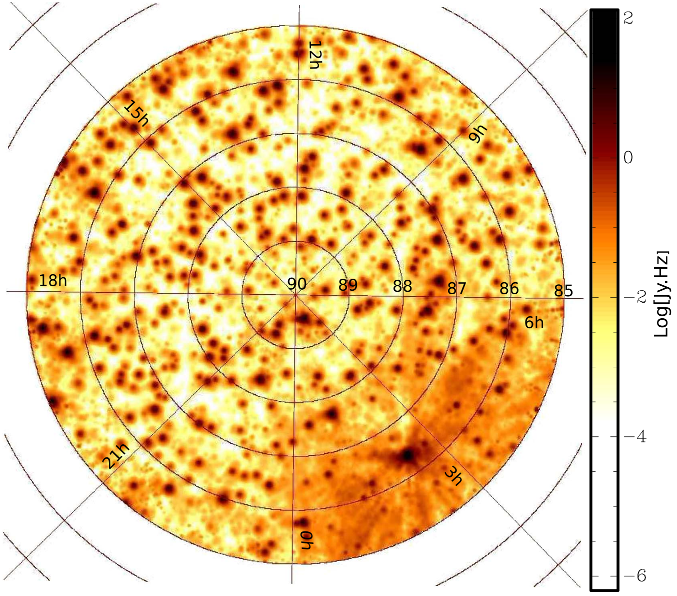

Figure 18. Reference 75 – 175 MHz CLEAN-ed image of north celestial pole (Q. Zheng et al. 2016), data from 40 stations

3. Beamform

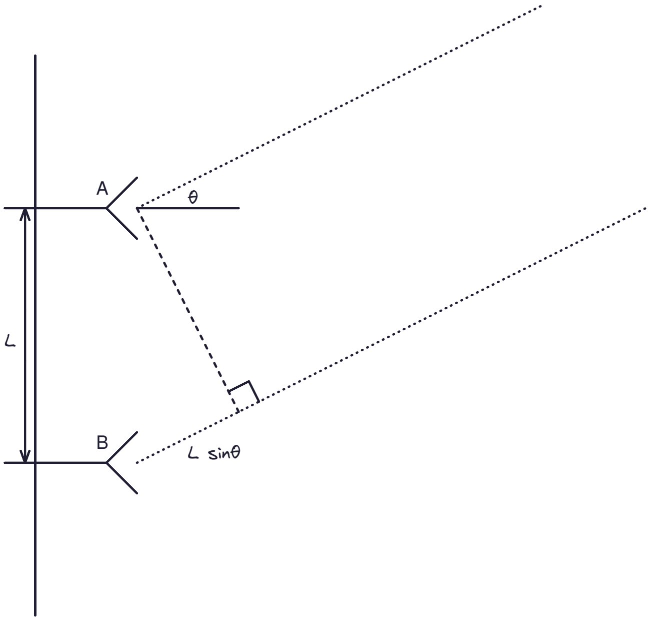

Figure 19. Schematic of beamform

3. Beamform

Sky intensity distribution

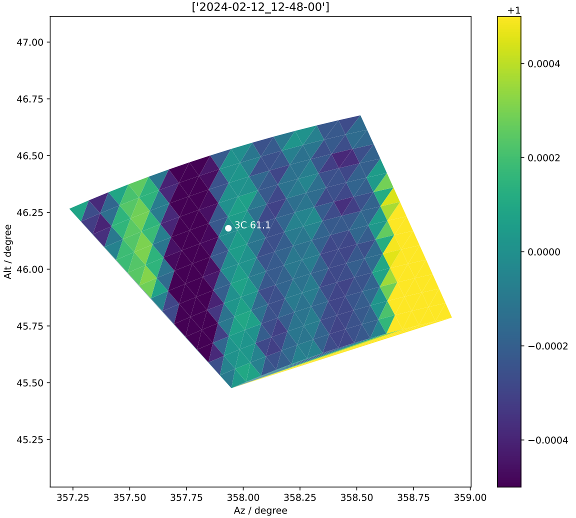

(a) 2024-02-12_12-48-00

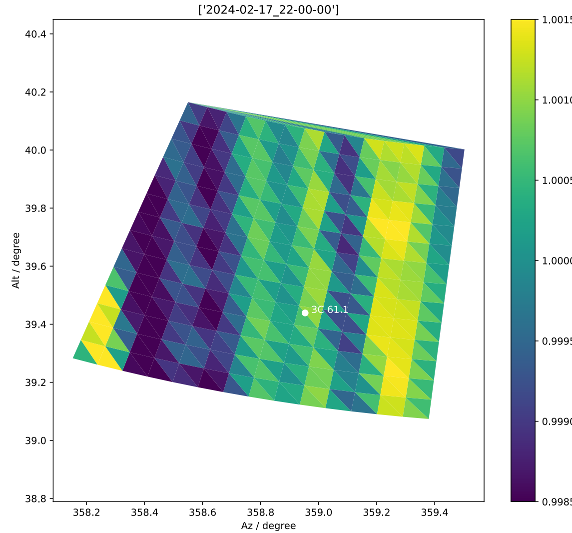

(b) 2024-02-17_22-00-00

Figure 20. Sky intensity distribution of several observations by beamforming, coordinate transformed to Altitude-Azimuth coordinate. White point represents 3C 61.1.

3. Beamform

Sky intensity distribution

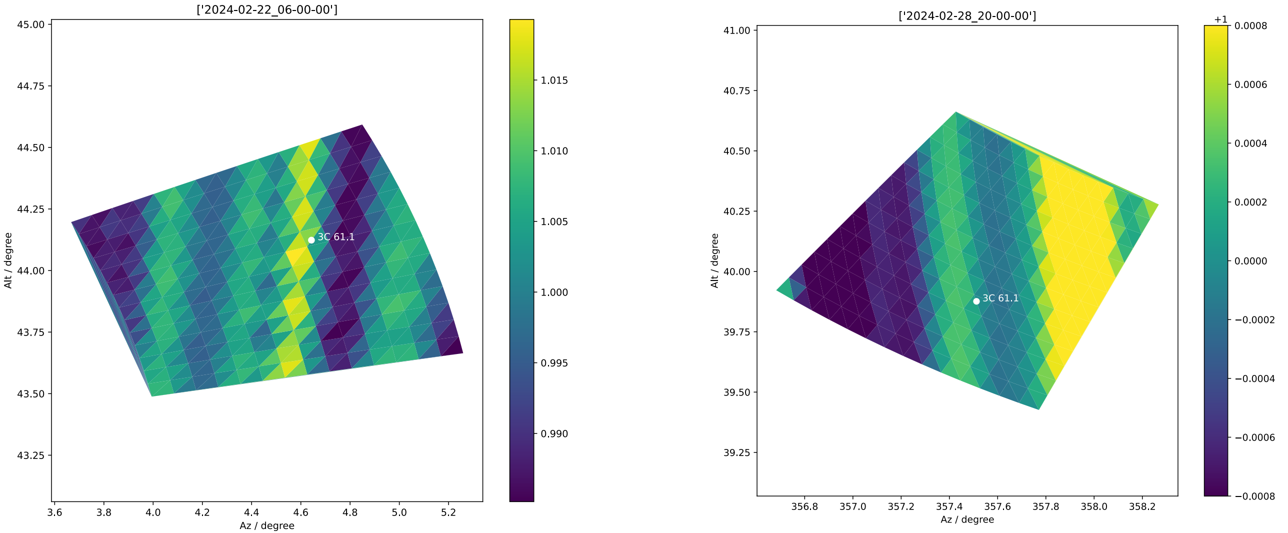

(a) 2024-02-22_06-00-00

(b) 2024-02-28_20-00-00

Figure 21. Sky intensity distribution of several observations by beamforming, coordinate transformed to Altitude-Azimuth coordinate. White point represents 3C 61.1.

3. Beamform

PSR B0329+54

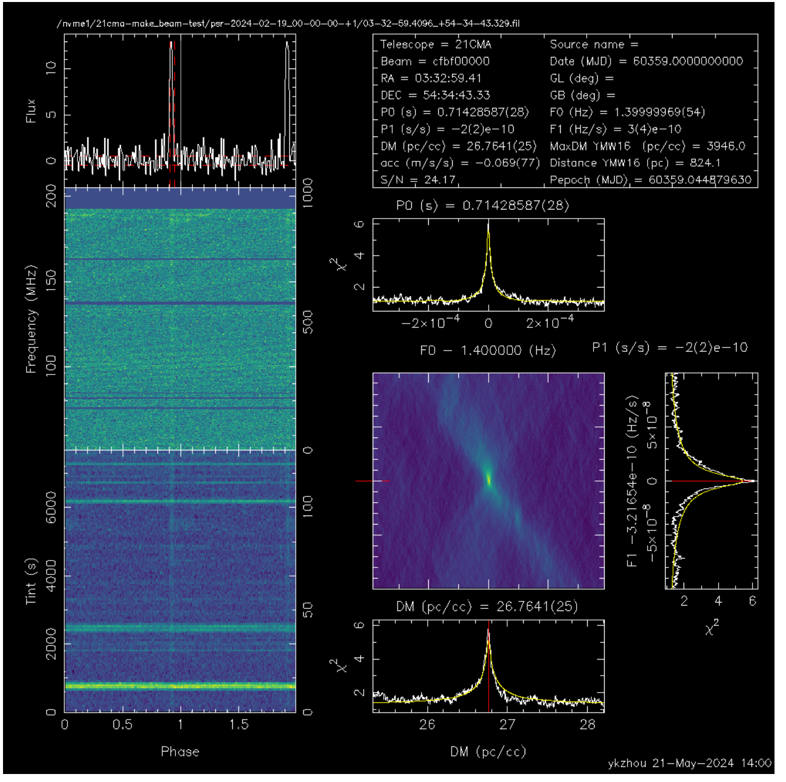

Figure 22. Observation 2024-02-19_00-00-00 (UTC) folded using PulsarX (Men et al. 2023a; Men et al. 2023b; Xu et al. 2022) targeting PSR B0329+54

3. Beamform

PSR B0329+54

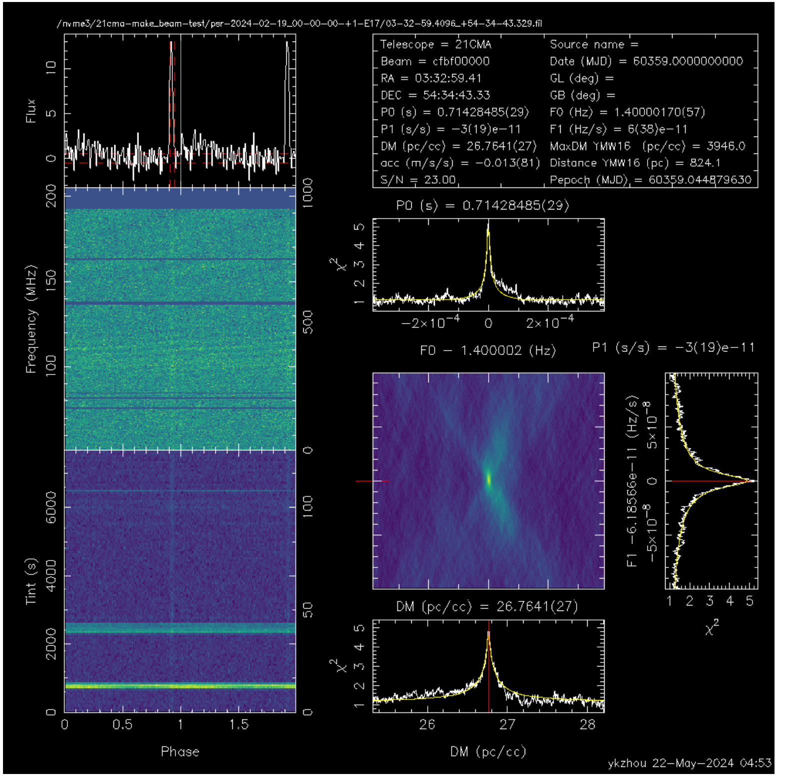

Figure 23. Observation 2024-02-19_00-00-00 (UTC) (E17 only) folded using PulsarX (Men et al. 2023a; Men et al. 2023b; Xu et al. 2022) targeting PSR B0329+54

4. Recent Work

Deployment of 6 more SNAPs

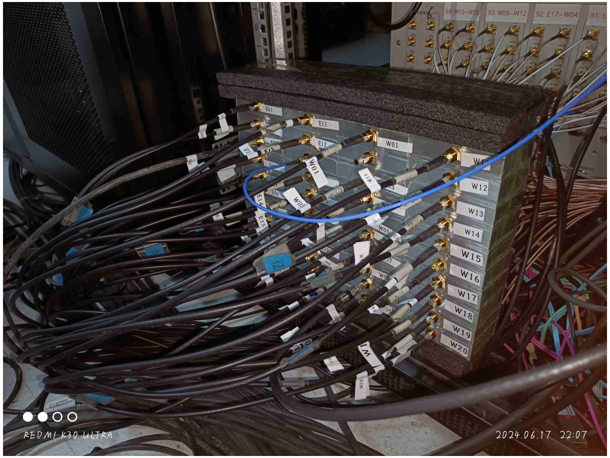

Figure 24. input signal wires

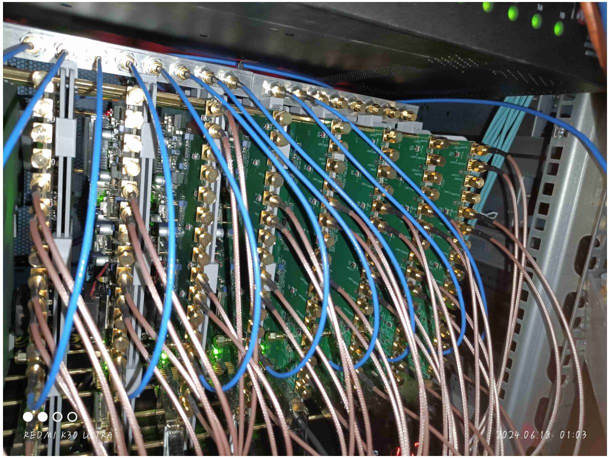

Figure 25. SNAPs with input signal connected

Conclusion & Plan

Done:

1. Deployed SNAP-based pulsar backend for 21CMA
2. Reproduced synthesis imaging of north celestial pole
3. Implemented beamformation for pulsar on 21CMA & observed PSR B0329+54

To do:

- Observe PSR J2351+8533
- Observe FRB 20240209A (Dec = +86d03m44.28s) (CHIME/FRB Collaboration 2024)
  - no burst detected yet...
- Implement distributed FX correlator based on GPU-like accelerators
- Implement distributed beamforming pipeline

Reference I

- CHIME/FRB Collaboration (2024). CHIME/FRB discovery of an active new repeating fast radio burst source FRB 20240209A. URL: https://www.astronomerstelegram.org/?read=16670.
- DeBoer, Dave et al. (2020). Smart Network ADC Processor (SNAP). URL: https://github.com/casper-astro/casper-hardware/blob/master/FPGA_Hosts/SNAP/README.md.
- Men, Yunpeng et al. (2023a). "PulsarX: A new pulsar searching package - I. A high performance folding program for pulsar surveys". In: A&A 679, A20. DOI: 10.1051/0004-6361/202347356. URL: https://doi.org/10.1051/0004-6361/202347356.
- Men, Yunpeng et al. (Dec. 2023b). PulsarX: Pulsar searching. Astrophysics Source Code Library, record ascl:2312.012.
- Thompson, A. R. (1999). "Fundamentals of Radio Interferometry". In: Synthesis Imaging in Radio Astronomy II. Ed. by Gregory B. Taylor, Christopher L. Carilli, and Richard A. Perley. Vol. 180. Astronomical Society of the Pacific Conference Series. Astronomical Society of the Pacific, pp. 11–36.

Reference II

Xu, H. et al. (Sept. 2022). "A fast radio burst source at a complex magnetized site in a barred galaxy". In: Nature 609.7928, pp. 685–688. ISSN: 1476-4687. DOI: 10.1038/s41586-022-05071-8. URL: https://doi.org/10.1038/s41586-022-05071-8.

Zheng, Cathie, Xiang-Ping Wu, and Melanie Johnston-Hollitt (2015). The NCP Region Observed with the 21 CentiMeter Array (21CMA). URL: https://leo.phys.unm.edu/~lwa/abq2015/talks/Zheng.pdf.

Zheng, Qian et al. (Feb. 2016). "Radio Sources in the NCP Region Observed with the 21 Centimeter Array". In: The Astrophysical Journal 832. DOI: 10.3847/0004-637X/832/2/190.

梁嘉一 (2024). "21CMA 脉冲星观测系统的延迟标定". MA thesis. 广州大学.

武向平 (2019). 中国 SKA 科学报告. 科学出版社.

Thank you!